

A review of anomalous refractive and reflective metasurfaces

Cite as: Nanotechnol. Precis. Eng. 5, 025001 (2022); <https://doi.org/10.1063/10.0010119>
Submitted: 12 January 2022 • Accepted: 12 March 2022 • Published Online: 18 April 2022

Siqi Liu, Zhenyu Ma, Jian Pei, et al.



View Online



Export Citation

ARTICLES YOU MAY BE INTERESTED IN

Vectorial metasurface holography

Applied Physics Reviews **9**, 011311 (2022); <https://doi.org/10.1063/5.0078610>

Tutorial on metalenses for advanced flat optics: Design, fabrication, and critical considerations

Journal of Applied Physics **131**, 091101 (2022); <https://doi.org/10.1063/5.0078804>

Design, fabrication, and measurement of reflective metasurface for orbital angular momentum vortex wave in radio frequency domain

Applied Physics Letters **108**, 121903 (2016); <https://doi.org/10.1063/1.4944789>



READ NOW!

AIP Advances
Nanoscience Collection

A review of anomalous refractive and reflective metasurfaces

Cite as: Nano. Prec. Eng. 5, 025001 (2022); doi: 10.1063/10.0010119

Submitted: 12 January 2022 • Accepted: 12 March 2022 •

Published Online: 18 April 2022



View Online



Export Citation



CrossMark

Siqi Liu,^{1,2,a)} Zhenyu Ma,^{1,b)} Jian Pei,^{1,2,c)} Qingbin Jiao,^{1,d)} Lin Yang,^{1,2} Wei Zhang,^{1,2} Hui Li,^{1,2} Yuhang Li,^{1,2} Yubo Zou,^{1,2} and Xin Tan^{1,3,e)}

AFFILIATIONS

¹Fine Instrument and Equipment R & D Center, Changchun Institute of Optics, Fine Mechanics and Physics, Chinese Academy of Sciences, Jilin 130033, China

²University of Chinese Academy of Sciences, Beijing 100049, China

³Center of Materials Science and Optoelectronics Engineering, University of Chinese Academy of Sciences, Beijing 100049, China

^{a)}Electronic mail: remiellsq@163.com

^{b)}Electronic mail: emozhai123@163.com

^{c)}Electronic mail: peijian980102@163.com

^{d)}Electronic mail: voynichjqb@163.com

^{e)}Author to whom correspondence should be addressed: xintan_grating@163.com. Tel.: 186 0431 1208

ABSTRACT

Abnormal refraction and reflection refers to the phenomenon in which light does not follow its traditional laws of propagation and instead is subject to refraction and reflection at abnormal angles that satisfy a generalization of Snell's law. Metasurfaces can realize this phenomenon through appropriate selection of materials and structural design, and they have a wide range of potential applications in the military, communications, scientific, and biomedical fields. This paper summarizes the current state of research on abnormal refractive and reflective metasurfaces and their application scenarios. It discusses types of abnormal refractive and reflective metasurfaces based on their tuning modes (active and passive), their applications in different wavelength bands, and their future development. The technical obstacles that arise with existing metasurface technology are summarized, and prospects for future development and applications of abnormal refractive and reflective metasurfaces are discussed.

© 2022 Author(s). All article content, except where otherwise noted, is licensed under a Creative Commons Attribution (CC BY) license (<http://creativecommons.org/licenses/by/4.0/>). <https://doi.org/10.1063/10.0010119>

KEYWORDS

Anomalous refraction and reflection, Generalized Snell's law, Metasurface material, Metalens

I. INTRODUCTION

Anomalous refraction and reflection, as the term implies, is a phenomenon in which, as a result of appropriate regulation of the wave direction of incident light, anomalous-angle or even negative-angle refraction occurs, and transmission and reflection do not satisfy Snell's law.¹⁻³ The main modulation methods currently available for the production of anomalous reflection and refraction are glass fiber arrays, three-dimensional metamaterials, and metasurface modulation. The glass fiber array method is based on the

principle of an optical waveguide and can achieve a negative refractive function of visible light and realize anomalous refraction within the scope of classical optics. However, this method is complicated and only single modulation is possible, and so it does not provide a basis for further development.⁴ With the use of three-dimensional metamaterials, flexible beam control can be achieved, but the complicated three-dimensional structures required to obtain complex optical functions increase the device size, posing obstacles to flattening and miniaturization.⁵⁻⁹ On the other hand, metasurfaces incorporating a subwavelength structure are able not only to

realize abnormal reflection and refraction, but also to alter the angle of reflection and state of polarization of outgoing light to enable such functions as electromagnetic wave front shaping. Because of these capabilities, metasurfaces have become an important topic of current research.^{10–12}

In 1621, the Dutch scientist Snell first provided a mathematical description of the phenomenon of light refraction at the interface between two media in what is now called Snell's law.³ On the basis of this law, a phase-matching theory was later derived according to which the electromagnetic wave vector components in the direction parallel to the interface are constants. Snell's law strictly constrains the angles of reflection and refraction. When the angle of incidence is known, together with the refractive indices of the media on each side of the interface, the angles of reflection and refraction can easily be calculated. Snell's law imposes limitations on the manipulation of light by conventional optical devices, owing to the uniform refractive index distributions of the materials from which such devices are constructed. Therefore, attempts have been made to use artificial metasurfaces to achieve arbitrary manipulation of light. An abrupt phase shift can be applied to an incident electromagnetic wave by a careful design of the metasurface microstructure. Anomalous refraction and reflection can be obtained according to Fermat's principle, and a generalization of Snell's law can be derived to describe this situation. If we assume that an abrupt phase shift $\Phi(x, y)$ is generated at a point (x, y) on the interface, then this generalized Snell's law can be expressed as

$$\begin{cases} n_i \sin \theta_r = n_i \sin \theta_i + \frac{\lambda_0}{2\pi} \frac{d\Phi}{dx}, \\ n_t \sin \theta_t = n_t \sin \theta_i + \frac{\lambda_0}{2\pi} \frac{d\Phi}{dx}, \end{cases} \quad (1)$$

where θ_i , θ_r , and θ_t are the angles of incidence, reflection, and refraction, respectively, while n_i and n_t are the refractive indices of the materials on the incident and refracted sides of the interface, respectively. Equation (1) lead to a modification of the expressions for phase matching, which become

$$\begin{cases} \vec{k}_r^{\parallel} - \vec{k}_i^{\parallel} = \nabla\Phi, \\ \vec{k}_t^{\parallel} - \vec{k}_i^{\parallel} = \nabla\Phi. \end{cases} \quad (2)$$

On the basis of these expressions, it is found that, in theory, the introduction of an abrupt phase shift Φ by the metasurface structure will enable a wider range of manipulations of light. By controlling the magnitude of the phase shift, it should be possible to change the amplitude and phase of light, as well as its direction of emission, thereby producing a variety of anomalous refractive and reflective phenomena. A number of different methods are currently being used to design and fabricate metasurfaces capable of producing anomalous refraction and reflection.

After more than a hundred years of development since Wood's discovery of anomalously reflected beams from subwavelength metal gratings in 1902, metasurfaces are now able to achieve modulation of electromagnetic waves in most spectral ranges. The design and application of anomalous refractive and reflective

metasurfaces have been realized from the microwave and terahertz (THz) bands, through the infrared (IR) part of the spectrum, to visible light. Compared with conventional optical components and metamaterial components, and the conventional optical lenses used in the cumulative phase method,¹³ metasurface structures are smaller. They do not need to be bent, and it is only necessary to employ a specially designed surface microstructure. Therefore, for example, metalenses constructed using anomalous refractive metasurfaces can facilitate the use of greatly simplified optical paths.^{14–16} Because of the planar geometry of metasurface, they take up less space than other components used for similar purposes, they are easier to manufacture, and they have a wider range of applications. Anomalous refractive and reflective metasurfaces now have practical uses in the military, scientific, and biomedical fields for such purposes as optical cloaking, wavefront shaping, and information transmission.^{17–21}

This paper summarizes the current state of development of anomalous refractive and reflective metasurfaces, focusing on two core issues, namely, tuning mode selection and the applications in different wavelength bands. It first describes the classification of anomalous refractive and reflective metasurface materials, then the progress that has been achieved in the application of anomalous refractive and reflective metasurface in different wavelength bands, and finally outlines the likely future development of these metasurfaces.

II. TYPES OF ANOMALOUS REFRACTIVE AND REFLECTIVE METASURFACES

Anomalous refractive and reflective metasurfaces, as functional components, can be classified as passive or active metasurfaces, depending on their tuning capabilities. Passive metasurfaces achieves their function through a fixed structure with a specific design and cannot be modulated. Active metasurfaces, on the other hand, combine metasurface structures with different sensitive units. Active tuning of such metasurfaces for incident electromagnetic waves can be achieved through the application of temperature, electricity, or light to expand their function or increase their bandwidth. In this section, the tuning modes of passively and actively tuned metasurfaces are compared and analyzed.

A. Passive metasurface tuning mode

Metasurface structures use optical antenna units to modulate light waves. In passive metasurfaces, metal antennas are usually used. An initial approach used a V-shaped Au antenna²² to add phase modulation to an incident light wave and thereby produce anomalous refraction and reflection of light. In a development of this method, as shown in Fig. 1(a), a double-layer metasurface structure was realized by combining a C-shaped Au antenna with an Si layer²³ and fabricating a grating on the back side, which significantly improved the efficiency of optical modulation in the THz band. It has even proved possible to integrate three metallic functional layers in a cascade of Au and dielectric layers to obtain a transmission–reflection dual-function structure.²⁴

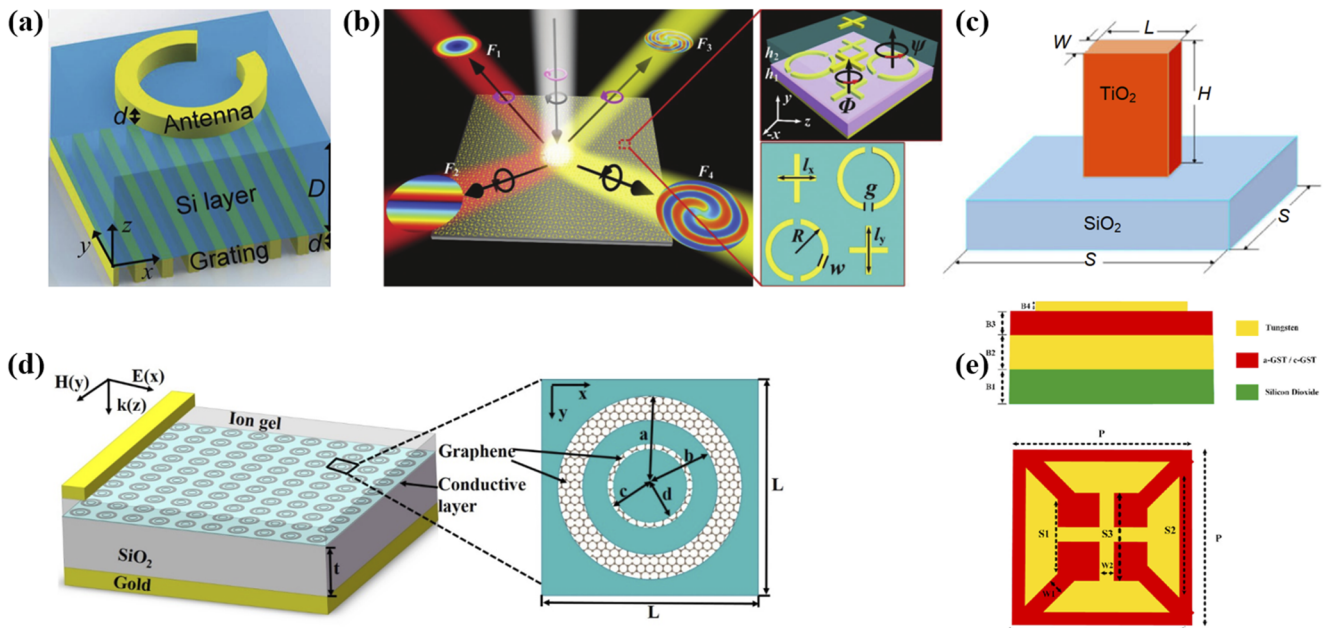


FIG. 1. Optical metasurfaces based on different tuning modes. (a) Cascaded multifunctional passive metasurface based on an Au antenna.²³ (b) Composite passive metasurface based on F4B dielectric and metal.²⁵ (c) All-dielectric passive metasurface based on TiO₂.²⁷ (d) Electrically controlled active metasurface based on graphene.³⁰ (e) Temperature-controlled active metasurface based on GST.³⁹

However, in high-frequency bands, the efficiency of a metasurface will be greatly affected by metallic dissipation at visible wavelengths, and therefore metasurface structures have been investigated in which only dielectric materials are used. For example, Xu *et al.*²⁵ have designed a composite metasurface formed from a combination of an F4B dielectric plate with a split ring resonator (SRR) and a crossbar metal patch, as shown in Fig. 1(b). This has a variety of potential applications in the microwave band. It is capable of generating orbital angular momentum and vortex light scattering in the frequency range of 7–14 GHz, in addition to anomalous refraction and reflection, and it can achieve up to 10 channels of beam modulation by encoding multiple wave vectors. It has been found that by exploiting the Pancharatnam–Berry (P-B) phase, a TiO₂ dielectric antenna integrated on an SiO₂ substrate can achieve high transmission efficiencies of 66%–83% in the 405, 532, and 660 nm bands.²⁶ By using similar materials for optical nanoantennas, as shown in Fig. 1(c), an anomalous refractive and reflective metasurface has achieved 71.3%–88.2% transmission efficiency in three bands in the 450–633 nm range.²⁷

Passive metasurfaces are designed with subwavelength antennas, and various types of tuning units can be formed by using different shapes and arrangements to achieve beam modulation for target light waves. At present, passive anomalous refractive and reflective metasurfaces are mainly prepared using metallic or all-dielectric materials. Metallic materials have reached a mature stage of development and are widely used, but they produce extremely high dissipation in the case of high-frequency light. All-dielectric materials can overcome this shortcoming of metallic

materials for near-IR and visible light, and they improve the transmission efficiency and working performance of metasurfaces, and they have therefore become the focus of research on metasurface materials.

B. Active metasurface tuning mode

Passive metasurfaces face many obstacles to practical application owing to the limitations imposed by their fixed structures. By contrast, actively modulated metasurfaces can be dynamically controlled by bringing in an external excitation source, and the materials used in their construction are selected according to their modulation modes. At present, there are three main metasurface driving methods, namely, electrical, optical, and thermal, which are summarized in this subsection.

Electrical modulation can be achieved in different ways. At microwave wavelengths, with a combination of a bottom metal layer and a PIN diode, it is possible to change the center frequency of the modulation and switch between transmission with the PIN off and reflection with it on.²⁸ In the microwave region, by combining a varactor diode and a metasurface microstructure, it is possible to realize anomalous refraction and reflection over a wide bandwidth through voltage regulation, and, by adding a horn-like structure, an incident wave can be transformed into a surface wave, thereby enabling dynamic functional switching with a wide bandwidth.²⁹ In the THz band, with the configuration shown in Fig. 1(d), in which a graphene-based metasurface is separated from an Au electrode by a thin SiO₂ layer, it is possible to adjust the operating bandwidth of the

metasurface by modulating the Fermi energy level of the graphene.³⁰ In another approach, Lee *et al.*³¹ used liquid crystals as electrically sensitive materials integrated with a V-shaped metasurface, which was fabricated by a focused ion beam technique, thereby providing an optoelectronic switch with reflection and refraction switching in the near-IR region.

In the case of light modulation, a photosensitive material is combined with a metasurface to achieve modulation. Photosensitive semiconductor materials are widely used in this modulation method. For example, by combining a GaAs substrate with structured Cu cells to form an SRR array and using an electromagnetic drive for the switching of a light-controlled metasurface, it is possible to achieve electromagnetic wave transmission and cutoff in the THz band.³² As another example, an optically modulated metasurface capable of light wave splitting has been fabricated using an Si substrate and Al structural units combined into an SRR array.³³

Thermal modulation takes advantage of the different crystal phase structures of thermally sensitive materials at different temperatures, which can produce changes in conductor/insulator properties. “On” and “off” functions have been studied from the THz to the visible bands. Li *et al.*³⁴ used an alternating combination of VO₂ and Cr separated by polyimide layers to form a metal-insulator-metal (MIM) resonator structure in the THz band. This bifunctional metasurface is able to act as a metalens, deflecting a beam when the VO₂ is in the insulating state, and transforming into an absorber when it is in the metallic state. In another application of the thermal phase-change material VO₂, a sandwich structure with Si and Au was fabricated in the far-IR band to accomplish the dual functions of absorption and beam control.³⁵ A VO₂-based metasurface has also been used in a multifunctional design at visible wavelengths.³⁶ Another thermal phase-change material, GST-225 integrated with an Si substrate, can also be used to realize switchable reflection and absorption by a metasurface in the THz band, controlled by temperature changes.³⁷ Li *et al.*³⁸ investigated a temperature-controlled metasurface in the near-IR in which GST-225 formed a transition layer between an Au structure and an SiO₂ substrate, and they verified that this metasurface could be changed from an overcoupling state to a critical coupling state, thereby providing a basis for active tuning of an anomalous refractive and reflective metasurface. Figure 1(e) shows a metasurface construction for the visible band in which a W metasurface structural unit sits above a GST-225 layer, followed by a W metal layer that itself is on top of a SiO₂ substrate.³⁹ With this structure, it is possible to realize variable tuning of the transmission peak at 500–740 THz.

As mentioned above, anomalous refractive and reflective metasurfaces can be constructed from different materials, depending on the choice of modulation method and mechanism. There has been an evolution from the initially adopted passive modulation approach to an active one. In the case of passive tuning, metal or all-dielectric materials with high reflectivity and low scattering coefficients have usually been selected. For active tuning of metasurfaces, depending on the tuning method adopted, appropriate sensitive materials are selected with the aim of achieving a rapid tuning response. In addition, in contrast to low-frequency bands, in high-frequency bands, when selecting the metasurface material, it is also necessary to consider the structural scale and the difficulty of the fabrication process. Thus, in addition to the metasurface material itself, the structural design of the metasurface is also of critical importance.

III. APPLICATIONS OF ANOMALOUS REFRACTIVE AND REFLECTIVE METASURFACES IN DIFFERENT WAVELENGTH BANDS

The design of anomalous refractive and reflective metasurfaces is strongly dependent on the wavelength range of the incident electromagnetic waves. Different wavelengths require different choices of materials and different structural details. Metasurfaces can be classified into three groups, depending on the incident wavelength range to which they are to be applied: (1) the microwave band, (2) the THz band, and (3) the IR and visible bands. Various types of metasurface structure have been designed for application in these different wavelength ranges.

A. Applications in the microwave band

The microwave band ranges from 300 MHz to 300 GHz, with wavelengths ranging from 1 mm to 1 m, and it is characterized by high transmittance. Anomalous refractive and reflective metasurfaces in this band could be applied to military cloaking,^{40–42} communications,^{43,44} and focused heating.⁴⁵ According to the number of wavelengths that are modulated, microwave metasurfaces can be divided into two types: single-frequency-acting and multifrequency-acting.

A single-frequency-acting metasurface is a metasurface that achieves the same modulation effect for a single band of electromagnetic waves. As shown in Fig. 2(a), negative-refractive-index metasurface based on SRRs is able to perform narrow-bandwidth negative-refractive-index regulation in the microwave range of 13.6–14.8 GHz,⁴⁶ but it has a narrow scope of application. Lin *et al.*,⁴⁷ using a design based on the P-B phase, have made an important breakthrough in achieving a super-bandwidth reflected light anomaly in the range of 7.7–19.9 GHz for circularly polarized light, which solves the narrow-bandwidth problem with regard to applications. Their metasurface is able to modulate incident linear or elliptically polarized light and split a beam into two polarized beams with left and right rotation. It can be used as a low-loss polarization device. However, the frequencies considered in current research on microwave refractive metasurfaces are mostly below 40 GHz, and fewer metasurfaces have been designed for the W-band (75–110 GHz) commonly used in current automotive radar and 5G communications. As shown in Fig. 2(b), to fill this gap in W-band research, Huygens’ principle was used to design a microwave metasurface for applications above 40 GHz ignored by existing microwave metasurface designs.⁴⁸ This high-efficiency transmissive Huygens metasurface in the W-band achieves negative refraction at 70–95 GHz.

Multifrequency-acting metasurfaces are able to produce different modulation effects for two or even more electromagnetic waves incident at the same time and are thus able to perform filtering or beam splitting. Compared with single-frequency-acting metasurfaces, their information capacities and functionalities are greatly increased, thus reducing manufacturing costs and device size. The currently adopted approaches to achieving multifrequency modulation use either (1) passively tuned metasurfaces where the metasurface structure is designed directly to achieve simultaneous modulation of light at different frequencies or (2) actively tuned metasurfaces where the metasurface microstructure is adjusted by application of external control to change the tuning frequency

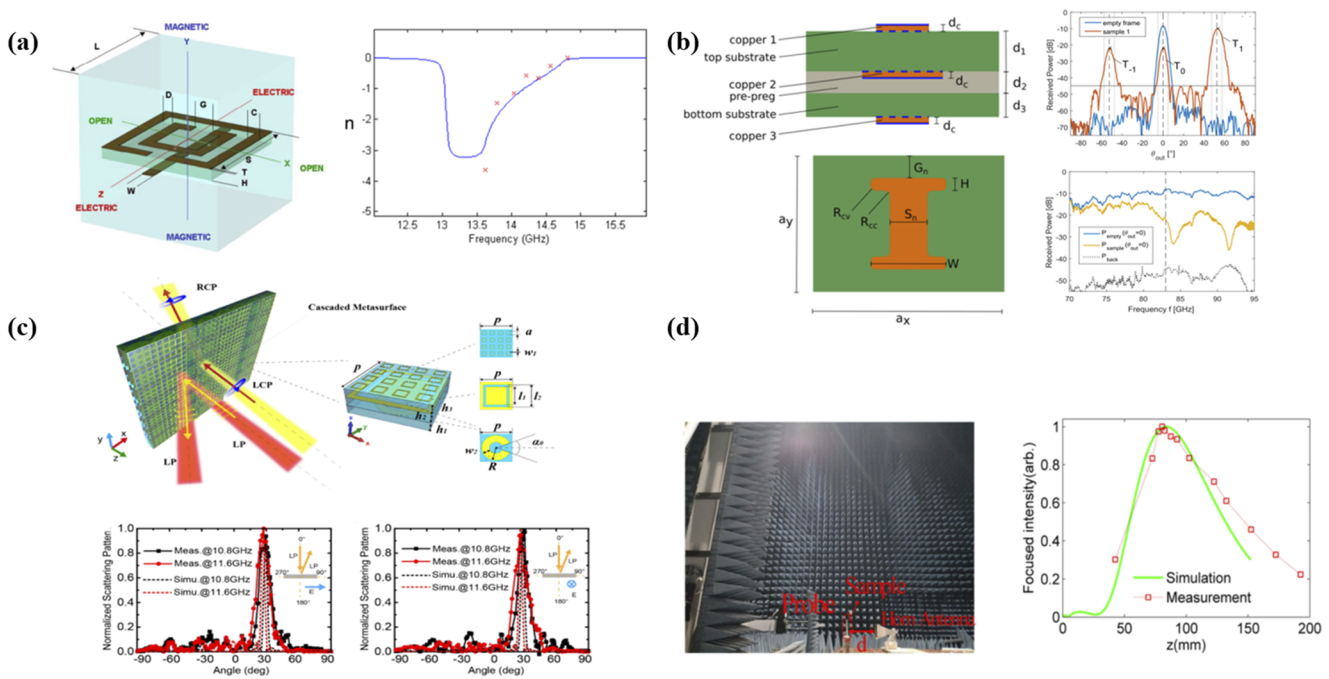


FIG. 2. Design of anomalous refractive and reflective metasurfaces in the microwave band. (a) Abnormal refractive and reflective metasurface based on an SRR array design.⁴⁶ (b) Huygens-type anomalous refractive and reflective metasurface in the W-band.⁴⁸ (c) Multifunctional abnormal refractive and reflective metasurface based on the P-B phase.²⁴ (d) Design of focusing metalens formed from a double-layer gradient metasurface.⁵⁴

or function. Among the latter, with the use of the generalized Snell's law, it is possible to design a three-dimensional single-crystal structure⁴⁹ to generate different reflection angles when two beams of orthogonally polarized light are incident at 18 and 32 GHz, and, in this way, filtering of electromagnetic waves at different wavelengths can be achieved with 98% reflective efficiency. On the basis of the P-B phase, Yang *et al.*²⁴ designed the cascaded metasurface shown in Fig. 2(c) for anomalous reflective and refractive modulation of left-handed polarized light in the 10.8–11.6 GHz band and of right-handed polarized light in the 6.0–6.3 GHz band, achieving good spectral characteristics. Through interference tuning of circularly polarized light, using a metasurface based on a double SRR with a concentric structure, absorption of left-rotation polarized waves and total reflection of right-rotation polarized waves were achieved, with a tuning efficiency of around 95%.⁵⁰ A Janus metasurface has been designed based on anomalous refraction and reflection, with a three-layer structure that expanded the available degrees of freedom, resulting in a six-channel function with an efficiency of about 75% in the microwave band.⁵¹ In this structure, two surfaces generate two asymmetric anomalous reflection channels each at wavelengths λ_1 and λ_2 , with two anomalous refraction channels being generated at a wavelength λ_3 . This metasurface is capable of achieving completely independent anomalous refraction and reflection functions at different frequencies, polarizations, or angles, thus significantly enhancing functional diversity, albeit with considerable operational difficulties. A conformal metasurface with a moderate curvature has been constructed with a structure using a rotating Jerusalem

cross element for tuning, based on the P-B phase, which can phase-compensate any linearly polarized or circularly polarized light and anomalously reflect it back to a biplane wave.⁵² Its reflection efficiency reaches 82% in the 8–18 GHz band and it can serve as a foundation for the further development of conformal metasurfaces providing anomalous refraction and reflection functions.

Although multifunctional integration is possible for passive metasurfaces through methods such as same-layer metasurface design and multilayer anisotropic coding, once such a surface has been fabricated, it cannot be changed in response to actual conditions and needs. As shown in Sec. III, active tuning of a metasurface can be achieved by combining it with an active component, such as by adding a PIN diode to the middle of the metasurface.²⁸ In this case, by powering up and powering down the metasurface, it can be switched between refractive and reflective behavior in the 2.07–2.10 GHz band. Adopting a similar approach, Mao *et al.*⁵³ extended the application spectrum to achieve active tuning of a refractive and reflective metasurface in the 4.7–5.9 GHz range.

The properties of anomalous refractive and reflective metasurfaces can be exploited for applications to optical wave beam modulation. For microwaves, as shown in Fig. 2(d), 80% transmission efficiency was achieved using a wide-angle phase-gradient metasurface with a double-layer structure, which overcame the limitation of previous metasurface lenses that could only receive vertical incident light and achieved incident focusing below an angle of 40°, thereby extending the range of application of metasurface lenses.⁵⁴ As an antenna for directional reception of microwave signals,⁵⁵

an innovative metasurface lens has been designed that converts spherical electromagnetic waves into planar electromagnetic waves, improving the antenna gain and operating bandwidth.

In summary, the trend of development of anomalous refractive and reflective metasurfaces in the microwave band is toward high frequencies, ultrawide bandwidth, and multifunctionality. These metasurfaces can act as plane lenses to focus for microwaves, with applications in radar detection, 5G communication, and other fields.

B. Applications in the THz band

The THz band ranges from 0.3 to 30 THz and is used in 6G communications, security inspections,^{56,57} biomedicine,⁵⁸ and laminar microscopy.^{59,60} To meet the requirements of these applications, active modulation of anomalous refractive and reflective metasurface in the THz band is essential. Unlike the materials required for active modulation in the microwave band, the THz band requires a combination of metasurface and phase-change dielectric materials to achieve device functionality. Currently, thermal phase-change materials and graphene are the dominant materials, together with semiconductors,⁶¹ liquid crystals,^{62–64} and superconductors,⁶⁵ which are also capable of achieving tunable functionality.

In the device shown in Fig. 3(a), VO₂ is used as a thermal phase-change material combined with the metasurface.⁶⁶ At temperatures of 300 and 400 K, VO₂ undergoes transitions between insulating and metallic states, and by placing different types of metasurface at

each end of the phase-change material, both refractive and reflective metasurfaces are obtained in the range 0.44–1.4 THz. However, this integration of two types of metasurfaces is at the cost of greater thickness. To solve this problem, as shown in Fig. 3(b), incorporation of graphene into the metasurface enables anomalous refraction and reflection in the range 0.75–2 THz,⁶⁷ with active tuning being achieved by changing the Fermi energy without changing the microstructure. With this approach, the metasurface could be thin enough to allow its integration into portable devices. As shown in Fig. 3(c), Luo *et al.*⁶⁸ also used graphene in combination with a metasurface to produce anomalous refraction in the 4.26–4.69 THz band and were again able to achieve active tuning.

There have been a number of investigations of the possible use of anomalous refractive and reflective metasurfaces in a variety of applications. For example, it has been demonstrated experimentally that a metasurface-based lens in the THz band can produce different holograms in different planes with 85% transmission.²³ The double-layer structure of this metalens, consisting of C-shaped antennas and a metal grating, does not require strict alignment, reducing the cost required for device mounting and maintenance. This design can also be used as a basis for future miniaturization and integration of such THz devices. Another tunable metasurface in the THz band has two different modes, with the reflection mode providing polarization conversion of incident light, while the transmission mode achieves beam focusing.⁶⁶ This design can provide a foundation for the development of multifunctional metasurface devices.

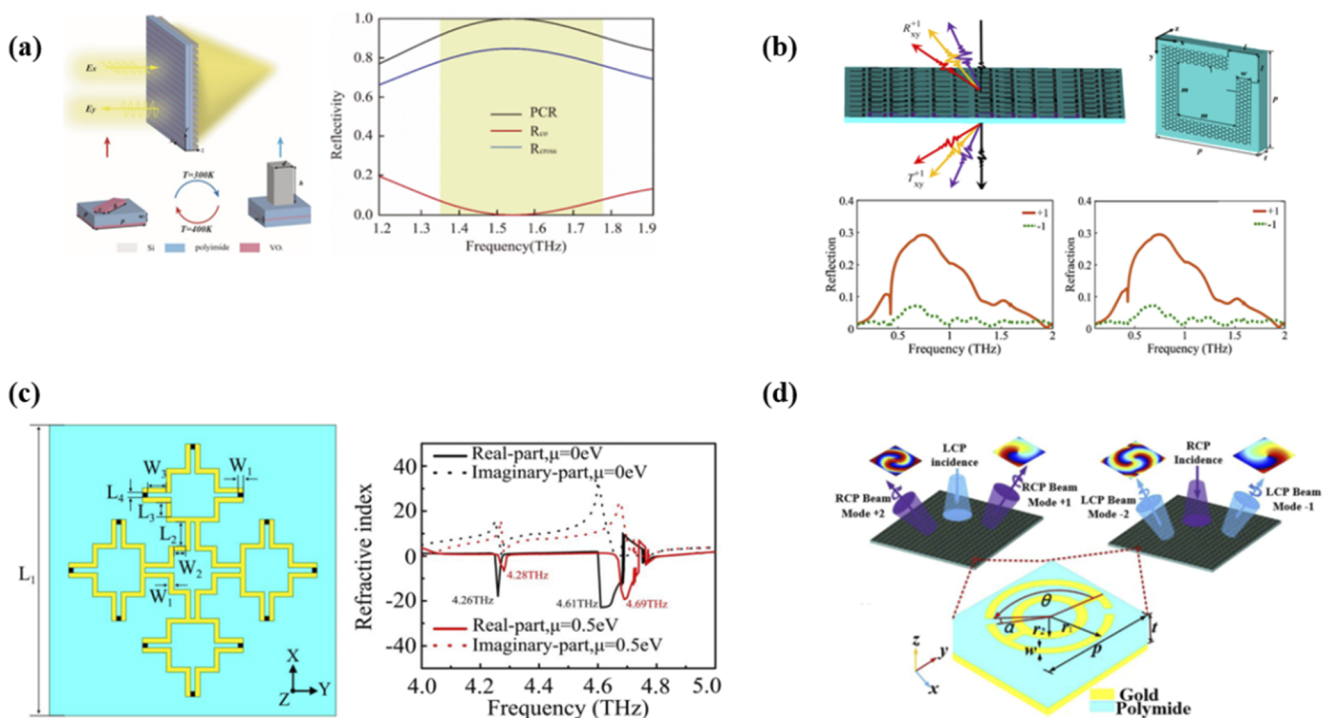


FIG. 3. Design of anomalous refractive and reflective metasurfaces in the THz band. (a) Application of a thermal phase-change refractive and reflective metasurface based on VO₂.⁶⁶ (b) and (c) Active anomalous refractive and reflective metasurfaces based on graphene.^{67,68} (d) Vortex beam generation based on a reflective metasurface.⁶⁹

According to the basic principle of phase tuning of a metasurface, an appropriate design of the metasurface structure will enable tuning of the reflection and transmission processes of a light wavefront in such a way that orbital angular momentum (OAM) is generated. Encoding of information in OAM of light can theoretically increase information capacity indefinitely. Therefore, in the THz band, a reflective metasurface was used to tune circularly polarized light, generating two types of vortex light in the 0.3–0.45 THz band in a simple and effective means of OAM generation,⁶⁹ as shown in Fig. 3(d). Shi and Zhang⁷⁰ used a multilayer graphene structure designed as a reflective metasurface that can form vortex light in the $l = \pm 1 - l = \pm 3$ mode. By tuning the Fermi energy, it was possible to tune the OAM beam in the range of 1.8–2.8 THz. Another approach to realize a tunable OAM generator is by combining a transmissive metasurface with the thermal phase-change material VO₂,⁷¹ which enables the tuning frequency to be manipulated by controlling the state of the VO₂ through temperature. A diffraction-free OAM beam can thereby be generated, with tuning being achieved without any need to change the physical structure. A three-layer metallic structure has been used to fabricate a transmissive metasurface that provides $l = \pm 1$, $l = \pm 2$, and $l = \pm 3$ modes of vortex light in the

0.3–0.9 THz range.⁷² Using an SRR and a structured phase-gradient metasurface will allow simultaneously modulation of the transmission and reflection of vertical incident bicircularly polarized light at THz wavelengths to produce two sets of vortex light in reflection and transmission,⁷³ thereby realizing the generation of vortex beams in transmission and reflection modes and overcoming the limitations of previous metasurfaces, which only provide either transmission or reflection functions, and expanding the electromagnetic tuning space.

Thus, active tuning of metasurfaces in the THz band has been achieved through the integration of thermal phase-change materials or graphene, thereby providing tuning of anomalous refraction and reflection. The use of thermal phase-change materials enables fast reversible tuning, but this is limited to two-state discrete tuning. With graphene, continuous electronically controlled tuning is possible, but the tuning range is small compared with that obtained with thermal control. Materials such as GST^{74,75} and GaAs⁶¹ can also be applied to the tuning of THz and IR–THz bands to achieve multifunctional integration. The next development goal in this area is the ability to achieve continuous multipoint modulation in the THz band with a large tuning range of anomalous refraction and

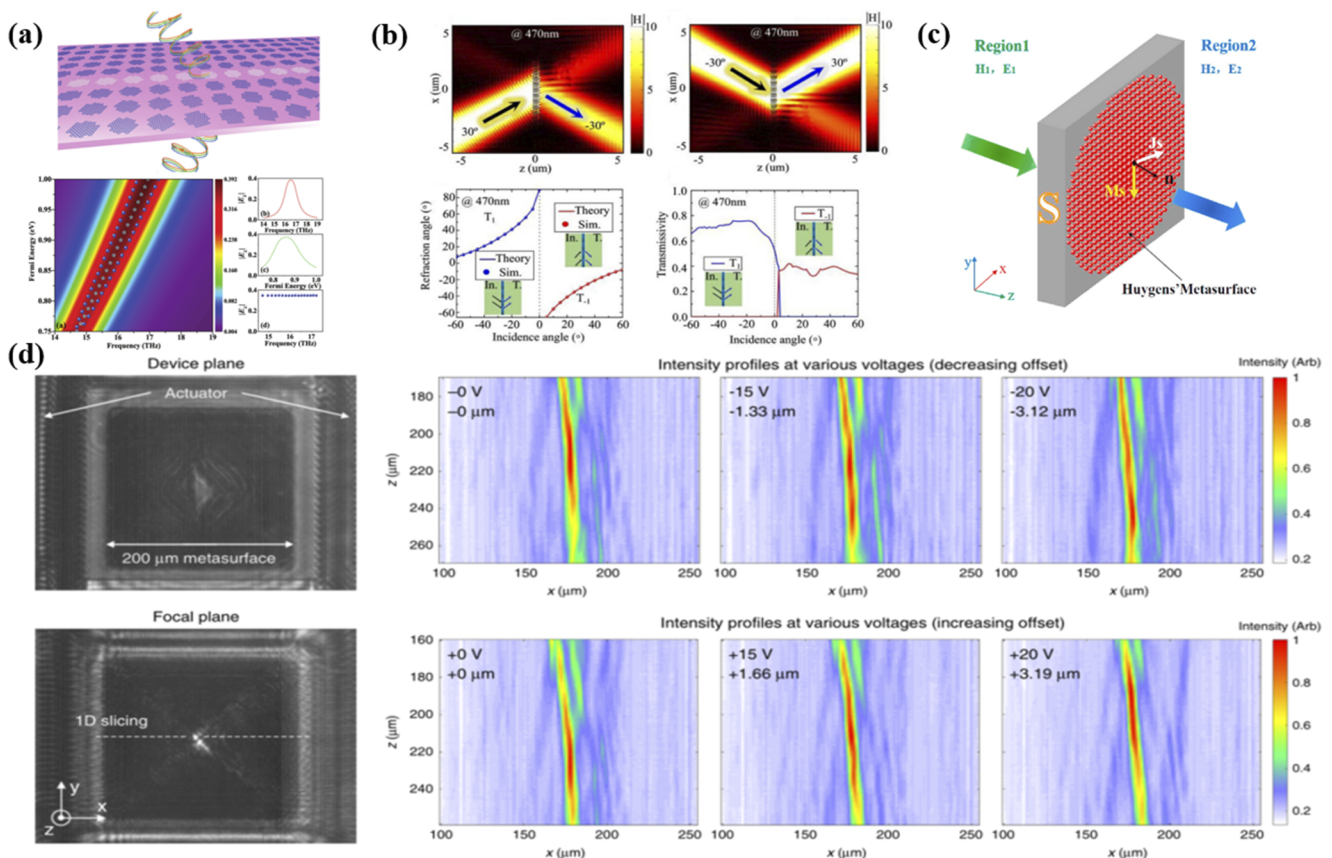


FIG. 4. Design of anomalous refraction and reflection metasurfaces in the IR and visible bands. (a) Metasurface designed on the basis of the P-B phase.⁷⁸ (b) Metasurface with a high-contrast design.⁸⁰ (c) Metasurface with a Huygens design.⁸¹ (d) Adjustable metalens structure incorporating an abnormal refraction and reflection metasurface and MEMS technology.⁸²

reflection. Another important direction of research in the THz band concerns the development of metasurface lenses and the generation of light with OAM light using anomalous refractive metasurfaces, with a wide range of potential applications in the fields of quantum information, optical communication, etc.^{70,76}

C. Applications in the IR and visible bands

The IR and visible wavelength bands range from 450 to 1 mm. In this wavelength range, high-frequency electromagnetic waves are strongly dissipated in metals,⁷⁷ which poses a major obstacle to the design of metasurfaces. However, all-dielectric metasurfaces with low Ohmic loss and high transmittance offer a solution to this problem and are key to the generation of anomalous refraction and reflection. All-dielectric metasurfaces can be broadly classified into three categories: P-B phase modulation metasurfaces, high-contrast metasurfaces, and Huygens metasurfaces.

In the all-dielectric design shown in Fig. 4(a), a P-B phase-based graphene metasurface produces anomalous reflection of circularly polarized light in the IR region.⁷⁸ In an example of the second approach, a topological algorithm was used to design a high-contrast metasurface incorporating a silicon-based wavelength grating.⁷⁹ Anomalous refraction was achieved in the visible and near-IR regions, with an efficiency reaching 60%–90%. Taking advantage of the high refractive index of SiGe in the visible region,⁸⁰ the phase gradient grating shown in Fig. 4(b) was able to achieve negative refraction in the range from 400 to 470 nm. The Huygens metasurface design scheme shown in Fig. 4(c), which was proposed by Tian *et al.*,⁸¹ uses disk-shaped nanoparticles, and it was able to achieve optical negative refraction at 1.32 μm and a transmittance of about 70% in the near-IR band. Compared with the first two types of all-dielectric metasurface, Huygens metasurfaces are easier to prepare, and the experimental results cited here demonstrate that they have great promise in the field of ultrathin optical lenses and optical chips.

A variety of applications have been proposed for anomalous refractive and reflective metasurfaces in the IR and visible bands. Column and aspheric lenses have been designed using all-dielectric Huygens metasurfaces.⁸¹ Transmission efficiencies of 73% and 68%, respectively, have been achieved at 1.32 μm , and the low aspect ratios of these lenses make them easy to fabricate and enable their application in compact precision devices such as those for hyperspectral imaging and in high-energy lasers. Figure 4(d) shows a metasurface lens combined with microelectromechanical systems (MEMS) technology.⁸² It uses a variable-focal-length conformal lens mechanism to achieve a focal shift at 1.55 μm incident wavelength. Aieta *et al.*⁸³ designed a metasurface that could be considered as a three-wavelength achromatic lens and, unlike previous achromatic elements, was not thick, complex, and costly. They were able to overcome the chromatic aberration produced by previous refractive and diffractive lenses. The excellent performance of this lens allows its application in a near-IR compact spectrometer.

The above three types of all-dielectric metasurfaces use different principles to realize anomalous refraction and reflection in the IR and visible bands. Compared with metallic materials, metasurfaces made of all-dielectric materials have high transmission efficiency and can realize high-band light focusing and achromatic planes, making them suitable for a variety of applications. However,

technical limitations mean that most such metasurfaces currently suffer from narrow bandwidth and relatively low efficiency. Also, because of manufacturing difficulties, many studies have only conducted theoretical simulations without experimental testing, which means that it is impossible to verify the results of these simulations. Therefore, key problems remain with regard to how the transmission spectra of these refractive and reflective metasurfaces can be broadened, how their transmission efficiencies can be improved, and how their fabrication can be made easier and cheaper.

IV. OUTLOOK FOR ANOMALOUS REFRACTIVE AND REFLECTIVE METASURFACES

A. Prospects for multifunctional anomalous refractive and reflective metasurfaces

Today, the development of anomalous refractive and reflective metasurfaces is moving toward multifunctionality, integration, and conformality. For passive refractive metasurfaces, a double-sided nanostructure design will enable multifunctional, wide-bandwidth and multi-angle electromagnetic wave tuning. By designing different metastructures on the two sides of such a metasurface and using an information-encoding design for the nanostructure, multifunctional modulation under different polarization conditions, wavelengths, and angles of incidence can greatly expand both functionality and degrees of freedom. For active anomalous refractive metasurfaces, the use of active or nonlinear materials can allow dynamical control of surface morphology and functionality. The functionality and operability of anomalous refractive and reflective metasurfaces can be enhanced by the use of a cascade of metasurfaces together with a phase-change material through which functional switching can be realized by the application of an external excitation.

However, there remains much scope for the further development of multifunctional anomalous refractive and reflective metasurfaces. For example, multiple-degree-of-freedom coupling is still a very complex process when considering the design of metasurfaces with a two-sided microstructure. Other important areas of potential research include the exploration of new materials suitable for use in dynamic multifunctional metasurfaces, the refinement of optical antenna fabrication processes, and methods for the alignment of cascaded metasurfaces. Further efforts are also needed to improve the efficiency of these devices, the signal-to-noise ratios of the images obtained, and the dynamic tuning rate.

B. Prospects for the application of anomalous refractive and reflective metasurfaces

Anomalous refractive and reflective metasurfaces have a wide variety of exciting possible applications. They are capable of generating vortex beams by wavefront shaping, which is a critical aspect of encrypted communication, and there is a current trend to integrate metasurfaces into multichannel vortex beam schemes. Through encoding of nanostructured arrays of metasurfaces, a multiplexing technique is used to split the information contained in different incident signals, which are resolved in different channels of the metasurface and then outputted. Such a design is able to significantly increase information capacity and is likely to become widely adopted.

In the field of holography, there are important roles for these metasurfaces in interferometry, stereo imaging, medical detection,

and image datafication. Reversing the design of an anomalous refractive and reflective metasurface and encoding polarization or phase information can create more degrees of freedom and expand information capacity, thereby overcoming the disadvantages of diffraction multilevel interference, small fields of view, and narrow bandwidth that arise in the conventional case, as well as greatly reducing noise in images.

There are also various directions for the development of anomalous refractive and reflective metasurfaces in the field of electromagnetic wave shielding and military stealth. On the one hand, by enabling absorption and anomalous reflection of incident electromagnetic waves, these metasurfaces can significantly reduce reflected radar waves and enhance stealth capability. On the other hand, flexible metasurfaces have become an interesting topic of research, in particular with regard to methods for enhancing their robustness. Their flexibility will broaden the range of applications of anomalous refractive and reflective metasurface by enabling their attachment to uneven surfaces.

V. CONCLUSION AND OUTLOOK

This paper has reviewed the progress of research on anomalous refractive and reflective metasurfaces. The driving modes of these metasurfaces have been described, they have been classified in terms of wavelength bands, methods for their structural design have been compared, and scenarios for their application in different bands have been described. Finally, the prospects for application of anomalous refractive and reflective metasurfaces have been presented, and directions for future research have been outlined.

However, despite the encouraging developments in metasurface technology, many problems and obstacles remain. For example, challenges remain regarding how precise regulation of electromagnetic waves on a metasurface can be ensured to achieve multifrequency co-regulation. The search for new dielectric materials to enable different ways of tuning and new functions of these metasurfaces is another important task. In the visible region, narrow bandwidth and low conversion efficiency impose limitations on regulation of metasurface functionality. In the context of experimental studies and practical applications, the problem arises that most of the current fabrication processes for metasurfaces are very cumbersome and do not lend themselves to mass production. Indeed, some theoretical metasurface models can only be simulated, and experimental test is unavailable. This presents an obstacle to the productization of metasurfaces. If the above problems can be solved, this will allow simplification of the design and fabrication processes and the realization of more powerful functions, leading to a wider range of applications for these metasurfaces in the military, communications, scientific, and biomedical fields.

ACKNOWLEDGMENTS

This work was supported by the Chinese Academy of Sciences Strategic Pioneering Science and Technology Special Project (XDA28050200), the Jilin Province Science and Technology Development Program in China (20200403062SF, 20200401141GX, 20210201023GX, 20210201140GX, and 20210203059SF), the Chinese Academy of Sciences Research Instrumentation Development Project (YJKYYQ20200048), and the Science

and Technology Innovation Platform of Jilin Province (20210502016ZP).

AUTHOR DECLARATIONS

Conflict of Interest

The authors have no conflicts to disclose.

DATA AVAILABILITY

Data sharing is not applicable to this article as no new data were created or analyzed in this study.

REFERENCES

- 1 McCall MW, Kinsler P, Favaro A, Censor D. What is negative refraction?. *Proc. SPIE* 2009;7392:73921M. <https://doi.org/10.1117/12.827472>.
- 2 Bolton HC. A history of physics in its elementary branches, including the evolution of physical laboratories. *J Am Chem Soc* 2002;21:714–715. <https://doi.org/10.1021/ja02058a017>.
- 3 Heavens OS. Principles of optics. By Born and Wolf. 1964. (Pergamon). *Math Gaz* 2016;49:485. <https://doi.org/10.2307/3612240>.
- 4 Ferrari JA, Frins E. Negative refraction and lensing at visible wavelength: Experimental results using a waveguide array. *Opt Express* 2011;19:13358–13364. <https://doi.org/10.1364/oe.19.013358>.
- 5 Chen L, et al. Dual-polarization programmable metasurface modulator for near-field information encoding and transmission. *Photonics Res* 2021;9:116. <https://doi.org/10.1364/prj.412052>.
- 6 Sun S, et al. High-efficiency broadband anomalous reflection by gradient metasurfaces. *Nano Lett* 2012;12:6223–6229. <https://doi.org/10.1021/nl3032668>.
- 7 Wong AMH, Eleftheriades GV. Perfect anomalous reflection with a bipartite Huygens' metasurface. *Phys Rev X* 2018;8:011036. <https://doi.org/10.1103/physrevx.8.011036>.
- 8 Zhang L, et al. Transmission-reflection-integrated multifunctional coding metasurface for full-space controls of electromagnetic waves. *Adv Funct Mater* 2018;28:1802205. <https://doi.org/10.1002/adfm.201802205>.
- 9 Zhao H, et al. Abnormal refraction of microwave in ferrite/wire metamaterials. *Opt Express* 2011;19:15679–15689. <https://doi.org/10.1364/oe.19.015679>.
- 10 Cui TJ, Liu S, Bai GD, Ma Q. Direct transmission of digital message via programmable coding metasurface. *Research* 2019;2584509. <https://doi.org/10.34133/2019/2584509>.
- 11 Ma Q, et al. Smart metasurface with self-adaptively reprogrammable functions. *Light Sci Appl* 2019;8:98. <https://doi.org/10.1038/s41377-019-0205-3>.
- 12 Wan X, Qi MQ, Chen TY, Cui TJ. Field-programmable beam reconfiguring based on digitally-controlled coding metasurface. *Sci Rep* 2016;6:20663. <https://doi.org/10.1038/srep20663>.
- 13 Yu N, Capasso F. Flat optics with designer metasurfaces. *Nat Mater* 2014;13:139–150. <https://doi.org/10.1038/nmat3839>.
- 14 Pendry JB. Negative refraction makes a perfect lens. *Phys Rev Lett* 2000;85:3966–3969. <https://doi.org/10.1103/physrevlett.85.3966>.
- 15 Wang W, et al. Far-field imaging device: Planar hyperlens with magnification using multi-layer metamaterial. *Opt Express* 2008;16:21142–21148. <https://doi.org/10.1364/oe.16.021142>.
- 16 Zhang X, Liu Z. Superlenses to overcome the diffraction limit. *Nat Mater* 2008;7:435–441. <https://doi.org/10.1038/nmat2141>.
- 17 Cao Y, Yu B, Fu Y, Gao L, Xu Y. Phase-gradient metasurfaces based on local Fabry-Pérot resonances. *Chin Phys Lett* 2020;37:097801. <https://doi.org/10.1088/0256-307x/37/9/097801>.
- 18 Ergin T, Stenger N, Brenner P, Pendry JB, Wegener M. Three-dimensional invisibility cloak at optical wavelengths. *Science* 2010;328:337–339. <https://doi.org/10.1126/science.1186351>.
- 19 Liu R, et al. Broadband ground-plane cloak. *Science* 2009;323:366–369. <https://doi.org/10.1126/science.1166949>.

- ²⁰Liu S, et al. Anisotropic coding metamaterials and their powerful manipulation of differently polarized terahertz waves. *Light Sci Appl* 2016;5:e16076. <https://doi.org/10.1038/lsa.2016.76>.
- ²¹Xu Y, Fu Y, Chen H. Planar gradient metamaterials. *Nat Rev Mater* 2016;1:16067. <https://doi.org/10.1038/natrevmats.2016.67>.
- ²²Yu N, et al. Light propagation with phase discontinuities: Generalized laws of reflection and refraction. *Science* 2011;334:333–337. <https://doi.org/10.1126/science.1210713>.
- ²³Zhao H, et al. High-efficiency terahertz devices based on cross-polarization converter. *Sci Rep* 2017;7:17882. <https://doi.org/10.1038/s41598-017-18013-6>.
- ²⁴Yang J, et al. Cascaded metasurface for simultaneous control of transmission and reflection. *Opt Express* 2019;27:9061–9070. <https://doi.org/10.1364/oe.27.009061>.
- ²⁵Xu HX, et al. Wavevector and frequency multiplexing performed by a spin-decoupled multichannel metasurface. *Adv Mater Technol* 2019;5:1900710. <https://doi.org/10.1002/admt.201900710>.
- ²⁶Khorasaninejad M, et al. Metalenses at visible wavelengths: Diffraction-limited focusing and subwavelength resolution imaging. *Science* 2016;352:1190–1194. <https://doi.org/10.1126/science.aaf6644>.
- ²⁷Wang D. All-dielectric metasurface beam deflector at the visible frequencies. *Opto-Electron Eng* 2017;44:103. <https://doi.org/10.3969/j.issn.1003-501X.2017.01.012>.
- ²⁸Tao Z, Wan X, Pan BC, Cui TJ. Reconfigurable conversions of reflection, transmission, and polarization states using active metasurface. *Appl Phys Lett* 2017;110:121901. <https://doi.org/10.1063/1.4979033>.
- ²⁹Xu HX, et al. Tunable microwave metasurfaces for high-performance operations: Dispersion compensation and dynamical switch. *Sci Rep* 2016;6:38255. <https://doi.org/10.1038/srep38255>.
- ³⁰Mou N, et al. Hybridization-induced broadband terahertz wave absorption with graphene metasurfaces. *Opt Express* 2018;26:11728–11736. <https://doi.org/10.1364/oe.26.011728>.
- ³¹Lee YU, Kim J, Wu JW. Electro-optic switching in metamaterial by liquid crystal. *Nano Convergence* 2015;2:23. <https://doi.org/10.1186/s40580-015-0054-6>.
- ³²Padilla WJ, Taylor AJ, Highstrete C, Lee M, Averitt RD. 2006 Conference on Lasers and Electro-Optics and 2006 Quantum Electronics and Laser Science Conference. 2006.
- ³³Cong L, et al. All-optical active THz metasurfaces for ultrafast polarization switching and dynamic beam splitting. *Light Sci Appl* 2018;7:28. <https://doi.org/10.1038/s41377-018-0024-y>.
- ³⁴Li X, et al. Switchable multifunctional terahertz metasurfaces employing vanadium dioxide. *Sci Rep* 2019;9:5454. <https://doi.org/10.1038/s41598-019-41915-6>.
- ³⁵Chen W, Chen R, Zhou Y, Ma Y. A switchable metasurface between meta-lens and absorber. *IEEE Photonics Technol Lett* 2019;31:1187–1190. <https://doi.org/10.1109/lpt.2019.2917439>.
- ³⁶Yang J-K, Jeong H-S. Switchable metasurface with VO₂ thin film at visible light by changing temperature. *Photonics* 2021;8:57. <https://doi.org/10.3390/photronics8020057>.
- ³⁷Liang L, Zheng Q, Nan X, Dong Y. Asymmetric all-dielectric active metasurface for efficient dual reflection modulation. *Opt Commun* 2022;505:127539. <https://doi.org/10.1016/j.optcom.2021.127539>.
- ³⁸Li C, Zhu W, Du S, Li J, Gu C. High-efficiency reflection phase tunable metasurface at near-infrared frequencies. *Chin Phys B* 2021;30:057802. <https://doi.org/10.1088/1674-1056/abe9a6>.
- ³⁹Patel SK, Charola S, Suresh Kumar R, Parmar J. Broadband polarization-insensitive Jerusalem-shaped metasurface absorber based on phase-change material for the visible region. *Physica B* 2022;624:413440. <https://doi.org/10.1016/j.physb.2021.413440>.
- ⁴⁰Cuesta FS, Asadchy VS, Mirmoosa MS, Tretyakov SA. 2018 12th International Congress on Artificial Materials for Novel Wave Phenomena (Metamaterials). 2018.
- ⁴¹Xu HX et al. Deterministic approach to achieve broadband polarization-independent diffusive scatterings based on metasurfaces. *ACS Photonics* 2017;5:1691–1702. <https://doi.org/10.1021/acsp Photonics.7b01036>.
- ⁴²Xu HX, et al. Deterministic approach to achieve full-polarization cloak. *Research* 2021:6382172. <https://doi.org/10.34133/2021/6382172>.
- ⁴³Tang W, et al. Wireless communications with programmable metasurface: Transceiver design and experimental results. *China Commun* 2019;16:46–61. <https://doi.org/10.23919/jcc.2019.05.004>.
- ⁴⁴Wang C, et al. Cylindrical vector beam multiplexing for radio-over-fiber communication with dielectric metasurfaces. *Opt Express* 2020;28:38666–38681. <https://doi.org/10.1364/oe.406300>.
- ⁴⁵Azad AK, et al. Ultra-thin metasurface microwave flat lens for broadband applications. *Appl Phys Lett* 2017;110:224101. <https://doi.org/10.1063/1.4984219>.
- ⁴⁶Gregor R, Parazzoli C, Li K, Koltenbah B, Tanielian M. Experimental determination and numerical simulation of the properties of negative index of refraction materials. *Opt Express* 2003;11:688–695. <https://doi.org/10.1364/oe.11.000688>.
- ⁴⁷Lin BQ, et al. Ultra-wideband anomalous reflection realised by a gradient metasurface. *IET Microwaves Antennas Propag* 2020;14:1424–1430. <https://doi.org/10.1049/iet-map.2020.0405>.
- ⁴⁸Olk AE, Macchi PEM, Powell DA. High-efficiency refracting millimeter-wave metasurfaces. *IEEE Trans Antennas Propag* 2020;68:5453–5462. <https://doi.org/10.1109/tap.2020.2975840>.
- ⁴⁹Hao H, Zheng S, Tang Y, Ran X. Design of dual-function metasurface based on beam polarization characteristics. *Opt Mater* 2021;117:111199. <https://doi.org/10.1016/j.optmat.2021.111199>.
- ⁵⁰Xu HX, et al. Interference-assisted kaleidoscopic meta-plexer for arbitrary spin-wavefront manipulation. *Light Sci Appl* 2019;8:3. <https://doi.org/10.1038/s41377-018-0113-y>.
- ⁵¹Xu HX, et al. Spin-encoded wavelength-direction multitasking Janus metasurfaces. *Adv Opt Mater* 2021;9:2100190. <https://doi.org/10.1002/adom.202100190>.
- ⁵²Xu HX, et al. High-efficiency broadband polarization-independent superscatterer using conformal metasurfaces. *Photonics Res* 2018;6:782. <https://doi.org/10.1364/prj.6.000782>.
- ⁵³Mao R, et al. Tunable metasurface with controllable polarizations and reflection/transmission properties. *J Phys D Appl Phys* 2020;53:155102. <https://doi.org/10.1088/1361-6463/ab6cd5>.
- ⁵⁴Liu YQ, Che Y, Qi K, Li L, Yin H. Design and demonstration of a wide-angle and high-efficient planar metasurface lens. *Opt Commun* 2020;474:126061. <https://doi.org/10.1016/j.optcom.2020.126061>.
- ⁵⁵Boubakri A, Choubeni F, Vuong TH, David J. A near zero refractive index metalens to focus electromagnetic waves with phase compensation metasurface. *Opt Mater* 2017;69:432–436. <https://doi.org/10.1016/j.optmat.2017.05.001>.
- ⁵⁶Nagatsuma T, Ducournau G, Renaud CC. Advances in terahertz communications accelerated by photonics. *Nat Photonics* 2016;10:371–379. <https://doi.org/10.1038/nphoton.2016.65>.
- ⁵⁷Dang S, Amin O, Shihada B, Alouini M-S. What should 6G be?. *Nat Electron* 2020;3:20–29. <https://doi.org/10.1038/s41928-019-0355-6>.
- ⁵⁸Siegel PH. Terahertz technology in biology and medicine. *International Microwave Symposium Digest*. 2004.
- ⁵⁹Lin H, et al. Investigation of pharmaceutical film coating process with terahertz sensing, optical coherence tomography and numerical modelling. 40th International Conference on Infrared, Millimeter and Terahertz Waves (IRMMW-THz). 2015.
- ⁶⁰Nagatsuma T, Ikeo T, Nishii H. 2013 21st International Conference on Applied Electromagnetics and Communications (ICECom). 2013.
- ⁶¹Liu S, et al. Resonantly enhanced second-harmonic generation using III-V semiconductor all-dielectric metasurfaces. *Nano Lett* 2016;16:5426–5432. <https://doi.org/10.1021/acs.nanolett.6b01816>.
- ⁶²Buchnev O, Podoliak N, Kaczmarek M, Zheludev NI, Fedotov VA. Electrically controlled nanostructured metasurface loaded with liquid crystal: Toward multifunctional photonic switch. *Adv Opt Mater* 2015;3:674–679. <https://doi.org/10.1002/adom.201400494>.
- ⁶³Decker M, et al. Electro-optical switching by liquid-crystal controlled metasurfaces. *Opt Express* 2013;21:8879–8885. <https://doi.org/10.1364/oe.21.008879>.

⁶⁴Wei BY, et al. Generating switchable and reconfigurable optical vortices via photopatterning of liquid crystals. *Adv Mater* 2014;26:1590–1595. <https://doi.org/10.1002/adma.201305198>.

⁶⁵Srivastava YK, Manjappa M, Krishnamoorthy HNS, Singh R. Accessing the high-Q dark plasmonic fano resonances in superconductor metasurfaces. *Adv Opt Mater* 2016;4:1875–1881. <https://doi.org/10.1002/adom.201600354>.

⁶⁶Li T, Wang H, Ling F, Zhong Z, Zhang B. High-efficiency terahertz metasurface with independently controlled and switchable function in transmission and reflection modes. *Superlattices Microstruct* 2020;146:106653. <https://doi.org/10.1016/j.spmi.2020.106653>.

⁶⁷Sun L, et al. Dynamically tunable terahertz anomalous refraction and reflection based on graphene metasurfaces. *Opt Commun* 2019;446:10–15. <https://doi.org/10.1016/j.optcom.2019.04.058>.

⁶⁸Luo Y, Zeng Q, Zhang X, Yan X, Xie W. 2019 Cross Strait Quad-Regional Radio Science and Wireless Technology Conference (CSQRWC). 2019.

⁶⁹Li J-S, Zhang L-N. Simple terahertz vortex beam generator based on reflective metasurfaces. *Opt Express* 2020;28:36403–36412. <https://doi.org/10.1364/oe.410681>.

⁷⁰Shi Y, Zhang Y. Generation of wideband tunable orbital angular momentum vortex waves using graphene metamaterial reflectarray. *IEEE Access* 2018;6:5341–5347. <https://doi.org/10.1109/access.2017.2740323>.

⁷¹Wang L, et al. Terahertz reconfigurable metasurface for dynamic non-diffractive orbital angular momentum beams using vanadium dioxide. *IEEE Photonics J* 2020;12:4600712. <https://doi.org/10.1109/jphot.2020.3000779>.

⁷²Zhang L, Li JS. Vortex beam generator working in terahertz region based on transmissive metasurfaces. *Optik* 2021;243:167452. <https://doi.org/10.1016/j.ijleo.2021.167452>.

⁷³Fan J, Cheng Y, He B. High-efficiency ultrathin terahertz geometric metasurface for full-space wavefront manipulation at two frequencies. *J Phys D Appl Phys* 2021;54:115101. <https://doi.org/10.1088/1361-6463/abcdd0>.

⁷⁴Holloway CL, Kuester EF. Generalized sheet transition conditions for a metascreen—A fishnet metasurface. *IEEE Trans Antennas Propag* 2018;66:2414–2427. <https://doi.org/10.1109/tap.2018.2809620>.

⁷⁵Jia X, Vahabzadeh Y, Caloz C, Yang F. Synthesis of spherical metasurfaces based on susceptibility tensor GSTCs. *IEEE Trans Antennas Propag* 2019;67:2542–2554. <https://doi.org/10.1109/tap.2019.2894036>.

⁷⁶Meng ZK, Shi Y, Wei WY, Zhang Y, Li L. Graphene-based metamaterial transmitarray antenna design for the generation of tunable orbital angular momentum vortex electromagnetic waves. *Opt Mater Express* 2019;9:3709. <https://doi.org/10.1364/ome.9.003709>.

⁷⁷Liu Y, Bartal G, Zhang X. All-angle negative refraction and imaging in a bulk medium made of metallic nanowires in the visible region. *Opt Express* 2008;16:15439–15448. <https://doi.org/10.1364/oe.16.015439>.

⁷⁸Cheng H, et al. Dynamically tunable broadband infrared anomalous refraction based on graphene metasurfaces. *Adv Opt Mater* 2015;3:1744–1749. <https://doi.org/10.1002/adom.201500285>.

⁷⁹Sell D, et al. Ultra-high-efficiency anomalous refraction with dielectric metasurfaces. *ACS Photonics* 2018;5:2402–2407. <https://doi.org/10.1021/acsp Photonics.8b00183>.

⁸⁰Wu Q, et al. Broadband optical negative refraction based on dielectric phase gradient metagratings. *J Phys D Appl Phys* 2021;54:445101. <https://doi.org/10.1088/1361-6463/ac1aa0>.

⁸¹Tian Y, Li Z, Xu Z, Wei Y, Wu F. High transmission focusing lenses based on ultrathin all-dielectric Huygens' metasurfaces. *Opt Mater* 2020;109:110358. <https://doi.org/10.1016/j.optmat.2020.110358>.

⁸²Han Z, Colburn S, Majumdar A, Böhlinger KF. MEMS-actuated metasurface Alvarez lens. *Microsyst Nanoeng* 2020;6:79. <https://doi.org/10.1038/s41378-020-00190-6>.

⁸³Aieta F, Kats MA, Genevet P, Capasso F. Multiwavelength achromatic metasurfaces by dispersive phase compensation. *Science* 2015;347:1342–1345. <https://doi.org/10.1126/science.aaa2494>.



Siqi Liu received the B.Eng. degree from Changchun University of Science and Technology in 2020 and is currently pursuing the Master's degree at Changchun Institute of Optics, Fine Mechanics and Physics, Chinese Academy of Sciences. His research interests include the design and fabrication of hyperspectral micro/nanodevices.



Zhenyu Ma received the Ph.D. degree from Changchun Institute of Optics, Fine Mechanics and Physics, Chinese Academy of Sciences, Changchun, China. His research interests include spectroscopic techniques.



Jian Pei received the B.Eng. degree from Changchun University of Science and Technology in 2020 and is currently pursuing the Master's degree at Changchun Institute of Optics, Fine Mechanics and Physics, Chinese Academy of Sciences. His research interests include the application and data analysis of hyperspectral imaging technology.



Qingbin Jiao received the Ph.D. degree from Changchun Institute of Optics, Fine Mechanics and Physics, Chinese Academy of Sciences, Changchun, China. His research interests include wet etching.



Xin Tan received the B.Eng. degree in 2003 and the Ph.D. degree in 2008 from the University of Science and Technology of China. He is currently professor at the Changchun Institute of Optics, Fine Mechanics and Physics, Chinese Academy of Sciences. His research interests include spectrometric instrumentation and the application of spectrometry to the development and application of micro/nano devices.